Photoionization Efficiency Curve Measurements of Alkali Metal Atom−Methyl Propiolate Clusters: Observation of Intracluster Cyclotrimerization Products

Hironori Tsunoyama, Fuminori Misaizu,* and Koichi Ohno*

Department of Chemistry, Graduate School of Science, Tohoku University, Aramaki, Aoba-ku, Sendai 980-8578, Japan

Received: March 18, 2004; In Final Form: May 18, 2004

Reaction products in clusters containing an alkali metal atom (M = Na, K, and Cs) and methyl propiolate (MP) molecules have been examined from results of photoionization efficiency (PIE) curve measurements. Two distinct humps were commonly observed in the PIE curves of $Cs(MP)_n$ for $n \geq 3$, whereas a relatively smooth curve was obtained for $n = 2$. In the photoionization mass spectra of $M(MP)_n$, an intensity anomaly at $n = 3$ was commonly observed as reported in the previous paper, which was due to a cyclotrimerization reaction producing a benzene derivative (trimethyl benzenetricarboxylate, BT). From the results of quantum chemical calculations for reacted and unreacted isomers, these two humps originate from two isomers with different ionization thresholds; the lower threshold is ascribed to a solvation-type isomer, $Cs(MP)_3$, and the higher value comes from a reacted isomer composed of a cesium atom and a BT molecule. From the relative intensity of two isomers, the intracluster cyclotrimerization reaction producing BT is found to proceed efficiently in the present M−MP clusters.

Introduction

The cyclotrimerization reaction of acetylene derivatives has received much attention as a method for the preparation of aromatic compounds.[1] This reaction has been extensively studied in the condensed phase[2−4] as well as on metal surfaces[5] from the pioneering work by Reppe and co-workers,[2] who suggested the metal-catalyzed mechanism of this reaction for the first time. In general, transition-metal complexes have been used as catalysts for this reaction. The mechanism of this reaction has received much attention in order to design new catalytic reagents and synthetic routes.[6] For this purpose, a molecular level study on the chemical reactions is important for elucidation of energetics and kinetics. Gas-phase studies of the chemical reactions have some advantages: (1) assignment and time evolution of the sequential reaction product are directly obtained from a mass spectrometric method and (2) size-dependent reactivity can be discussed without solvent effects.

Gas-phase studies of metal-mediated cyclotrimerization reaction of acetylene molecules have been performed by Schwarz and co-workers.[7,8] They were able to identify the cyclotrimerization in the $Fe^+-C_2H_2$ system by mass spectrometry and collision-induced dissociation measurements using a Fourier-transform ion cyclotron resonance apparatus.[7] In the gas-phase, metal-catalyzed benzene formation has also been reported in transition-metal ion−ethylene complexes.[9−11] This reaction was found to be composed of two steps: acetylene molecules were first produced sequentially via dehydrogenation of ethylene molecules by the metal cation (M^+), then the cyclotrimerization of acetylene proceeds in the $M^+(acetylene)_n$ complex. In recent years, Heiz and co-workers investigated a reactivity of palladium clusters deposited on a MgO(100) surface toward acetylene polymerization.[12] They found that the cyclotrimerization to form benzene molecules proceeds on palladium clusters and that this reaction is promoted by metal atoms or clusters on defect sites (oxygen vacancy) having anionic nature.[13]

Ionic polymerization is known to be another reaction with sequential coupling of unsaturated compounds. In the gas phase, ionic polymerization has been studied to some extent for acetylene derivatives[14,15] as well as for vinyl compounds.[16−28] Garvey and co-workers have studied intracluster reactions of acetylene and methyl acetylene cluster cations.[14] In the mass spectra of cluster ions of acetylene derivatives, $(HC{\equiv}CR)_n^+$, an intensity anomaly at $n = 3$ was commonly observed, which was explained by the intracluster cyclization producing a benzene derivative.[14] Formation of a covalently bonded cyclic molecule was also found in the acetylene−acetone heterocluster.[15] As for vinyl compounds, Kondow and co-workers have found that the cyclotrimerization reaction proceeds in the acrylonitrile (AN) cluster anions from the studies of mass spectrometry,[16] photodissociation,[17,18] collision-induced dissociation,[19] and photoelectron spectroscopy.[20,21] Similar intracluster reactions in alkali metal atom−vinyl compound clusters were also reported by the authors' group.[22−28] In the photoionization mass spectra of clusters containing an alkali metal atom (M = Li, Na, and K) and vinyl molecules (VM; AN, acrylic ester, methacrylic ester, methyl vinyl ketone), $M(VM)_n$, an intensity anomaly was commonly observed at $n = 3$.[22−26] This feature was explained by the cyclotrimerization reaction producing cyclohexane derivatives initiated by the alkali metal atom. In addition, intensity anomalies at $n = 3k$ ($k = 1-4$) were also found in the M−AN system,[22,23] which was explained by the sequential production of cyclohexane derivatives. In M−AN clusters, cyclohexane ring formation was confirmed by the size distribution of metastable dissociation from $K^+(AN)_n$ photoions,[22] photodissociation of the neutral clusters,[23] and negative-ion photoelectron spectroscopy.[27] On the other hand, there are few studies on the metal-mediated cyclotrimerization of acetylene derivatives in the gas-phase neutral systems; very recently, we reported the intracluster cyclization reaction in an alkali

* To whom correspondence may be addressed. E-mail: misaizu@qpcrkk.chem.tohoku.ac.jp (F.M.); ohnok@qpcrkk.chem.tohoku.ac.jp (K.O.).

10.1021/jp048803m CCC: $27.50 © 2004 American Chemical Society
Published on Web 06/22/2004

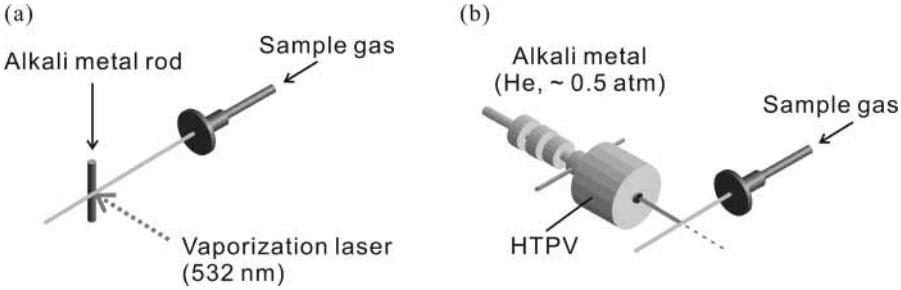

Figure 1. Schematic diagram of pick-up-type cluster sources of an alkali metal atom with MP molecules. (a) The laser vaporization type and (b) the high-temperature pulse valve. Both of the alkali metal sources were combined with pulsed supersonic jets of MP molecules.

metal atom−methyl propiolate molecule clusters produced by the laser vaporization method.[28]

In the present paper, we have further examined the intracluster reaction in clusters containing an alkali metal atom (M = Na, K, and Cs) and methyl propiolate molecules (MP; HC≡CCOOCH$_3$) from the results of photoionization efficiency (PIE) curve measurements and quantum chemical calculations based on density functional theory (DFT). We have determined ionization thresholds of Cs(MP)$_n$ (n = 2−6) from PIE curve measurements. From the comparison between theory and experiment, we have confirmed the benzene derivative formation by intracluster anionic polymerization and have found the coexistence of reacted and unreacted isomers. Furthermore, the relative abundance of the reacted isomer was also discussed. In addition, we have also examined the effects of a laser vaporization method on the intracluster reaction by comparing with another type of alkali metal source.

Experimental Section

The experimental apparatus was previously described in detail.[22] The apparatus is composed of three-stage differentially evacuated chambers that contain a cluster source and a reflectron-type time-of-flight mass spectrometer (TOF-MS). Clusters containing an alkali metal atom and MP molecules were produced by a pick-up source[29−31] with a combination of an alkali metal atom source using laser vaporization or a high-temperature pulse valve[32] and a pulsed supersonic jet. Schematic diagrams of the two types of cluster sources used in the present experiment are shown in Figure 1. In the laser vaporization source as shown in Figure 1a, the second harmonic output of a Nd:YAG laser was focused onto an alkali metal rod, which was translated and rotated so as to stabilize the vaporization condition. Generated alkali atoms were immediately collided with molecular clusters produced in the pulsed supersonic expansion via a pulse valve (General Valve, Series 9, orifice diameter 0.8 mm) at ∼10 mm downstream of the nozzle. The MP vapor mixed with helium buffer gas (Nihon Sanso, 99.9999% pure) was expanded from the pulse valve. Generated charged particles were removed by a static electric field after collimation with a conical skimmer (throat diameter of 3 mm). We also utilize a high-temperature pulse valve as shown in Figure 1b for the source of potassium and cesium atoms. This pulse valve can be heated to 500 °C, and the temperature of the valve was monitored by a thermocouple. The nozzle exit of the valve was usually kept at ∼320 °C for cesium, at which temperature the cesium vapor pressure is estimated to be 3.0 Torr. For the potassium case, the nozzle temperature and the vapor pressure were kept at ∼360 °C and 1.5 Torr, respectively. Alkali metal vapor was diluted by helium buffer gas of ∼0.5 atm. Produced alkali atoms were collided with the molecular clusters in the pulsed supersonic expansion region at ∼50 mm downstream from the nozzle of the molecular cluster source. In both sources, clusters containing only one metal atom were predominantly produced because of the low concentration of the metal atoms in the cluster generation region. Produced binary clusters were introduced into the TOF-MS chamber after the collimation by the conical skimmer.

The neutral clusters were ionized by irradiation with a pulsed laser beam in the acceleration region of the TOF-MS. Frequency-doubled output of a dye laser (Spectra-Physics, PDL-2 and Inrad, Autotracker III) pumped by a Nd:YAG laser (Spectra-Physics, GCR-150−10) was used as a photoionization light source. The laser fluence was kept under 4 mJ/cm^2 in order to avoid multiphoton processes. Photoions were accelerated to ∼3 keV by using Wiley−McLaren-type electrodes. These ions were reflected back to an ion detector by reflection electrodes after traveling a field-free region of ∼1100-mm length. After traveling the second field-free region (700-mm length), ions were detected by a dual microchannel plate (MCP, Hamamatsu Photonics, F1552-21S). Ion signals were averaged over 1000 laser shots at a given photoionization wavelength by a digital storage oscilloscope (LeCroy, 9344C), and the data were transferred to a personal computer via a GPIB computer interface. The ionization efficiency was obtained as the cluster ion intensity relative to that of the cesium atomic ion in order to reduce the fluctuation of the cluster source and of the ionization laser power. Obtained photoionization efficiency curves were also averaged over more than three independent measurements.

The sample rods of sodium (Rare Metallic, 99.9% pure) and potassium (Aldrich, 99.5% pure) were made under nitrogen atmosphere in a vacuum drybox (UNICO, UN650F) so as to avoid a reaction with water in the air. Potassium and cesium (Aldrich, 99.95% pure) were introduced to the high-temperature pulse valve also under nitrogen atmosphere in the vacuum drybox. The MP sample (Aldrich, 99%) was used without further purification.

Theoretical Calculations

Density functional calculations for M(MP)$_3$ (M = Na, K) clusters were performed in order to obtain ionization thresholds of the clusters. All calculations were carried out by using the Gaussian 98 program package.[33] The B3LYP functional[34] was utilized in conjunction with the 6-31G(d) basis set for H, C, O, and Na, and the 6-311+G(2d) basis set was used for K. The M(MP)$_3$ clusters were optimized for the structure with the highest symmetry, where each M−MP portion is similar to that of the most stable structure of a 1:1 complex reported previously.[28] For geometry optimization of the reaction product, which contains the alkali metal atom and the trimethyl 1,3,5-benzenetricarboxylate (BT) molecule, we start optimization from the most stable isomer of the BT molecule. Adiabatic ionization energies were obtained from an energy difference between the

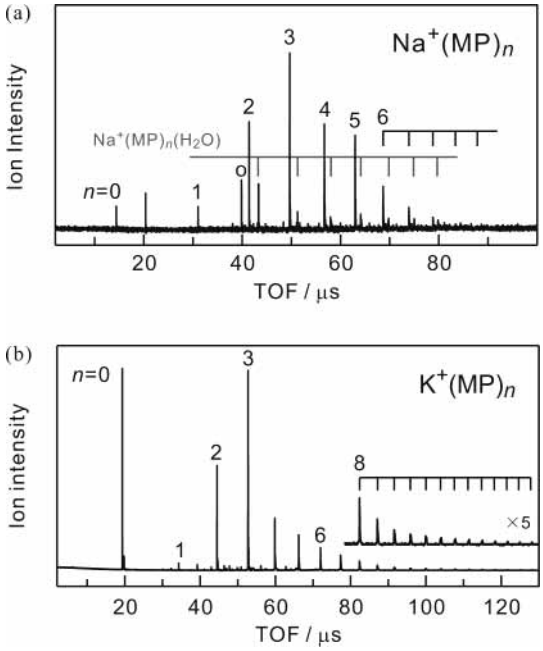

Figure 2. Typical photoionization mass spectra of (a) $Na(MP)_n$ and (b) $K(MP)_n$ obtained by 5.64-eV laser irradiation. These clusters were produced by a pick-up source with a combination of the laser vaporization and a pulsed supersonic jet. Fragment ions with a loss of CH_2 from $M(MP)_2$ was denoted by a circle.

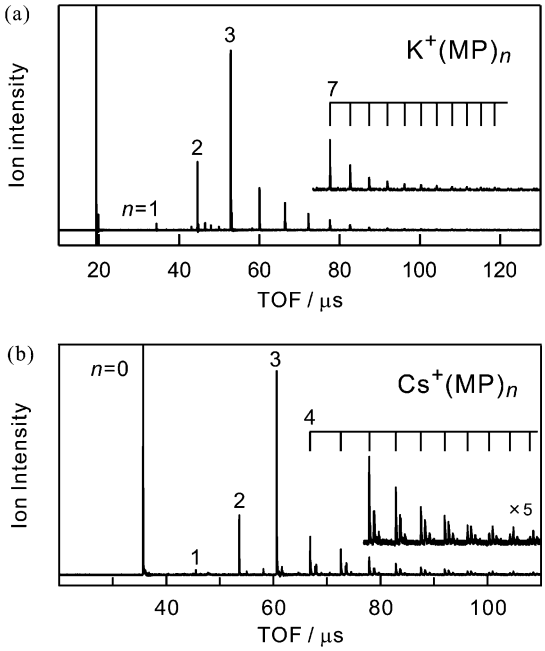

Figure 3. Typical photoionization mass spectra of (a) $K(MP)_n$ and (b) $Cs(MP)_n$ obtained by 5.64-eV laser irradiation. These clusters were produced by a pick-up source with a combination of the high-temperature pulse valve and a pulsed supersonic jet.

optimized neutral complex and the corresponding cation. We also estimated vibrational frequencies for both isomers from the frequency analysis. Obtained vibrational frequencies were used without multiplying any scaling factors.

Results and Discussion

A. Photoionization Mass Spectra. Typical photoionization mass spectra of $M(MP)_n$ (M = Na and K) clusters produced by the laser-vaporization source are shown in Figure 2. These mass spectra, obtained by one-photon ionization with a laser beam at 5.64 eV, were almost similar with the result in the previous paper;[28] an intensity anomaly at $n = 3$ was commonly observed in the sodium and potassium systems. In Figure 2a, cluster ion series of $Na^+(MP)_n$ was predominantly observed along with additional side peaks assignable to $Na^+(MP)_n(H_2O)$, which are due to water impurity in the MP sample. In Figure 2b, cluster ions of $K^+(MP)_n$ were mainly observed, and the side peaks of $K^+(MP)_n(H_2O)_m$ were hardly observed because of the absence of water impurity. In both systems, the cluster ions of $M^+(MP)_3$ were more abundant than adjacent cluster sizes. This feature was almost independent of the ionization energy ranging from 4.90 to 5.64 eV.

Figure 3 shows typical photoionization mass spectra of $M(MP)_n$ (M = K and Cs) generated by the source using the high-temperature pulse valve. In these mass spectra, cluster ion series of $M^+(MP)_n$ (M = K and Cs) was predominantly observed. In Figure 3b, several side peaks were also observed beside the large *n* clusters. These ions are probably due to some kind of impurity in the high-temperature pulse valve, although accurate assignment for these ions is not possible. In both mass spectra, the intensities of $Cs^+(MP)_3$ and $K^+(MP)_3$ ions were also higher than those of adjacent sizes, and this feature was commonly observed for the ionization laser energy from 4.90 to 5.64 eV. From the consideration of the relative stability of the neutral clusters, intensity anomaly at $n = 3$ was concluded to be due to intracluster cyclotrimerization reaction producing a BT molecule as discussed in the recent paper.[28] We measured PIE curves for $Cs(MP)_n$ clusters in order to confirm the benzene formation and to determine ionization thresholds for these clusters, as discussed in the next section.

B. Photoionization Efficiency Curves. Figure 4 shows PIE curves of $Cs(MP)_n$ ($n = 2-6$) clusters. These curves were obtained by plotting the $Cs^+(MP)_n$ intensity normalized by that of the Cs^+ ion in the same mass spectrum, to remove a fluctuation of the cluster source condition, as a function of ionizing photon energy. The ionization efficiency of $Cs(MP)_2$ increases monotonically with the photon energy as shown in Figure 4a. In contrast, two distinct rising steps were clearly observed for $n = 3-6$.

To explain this feature in PIE curves, we must consider two possible isomers: (i) an alkali metal atom solvated by MP molecules and (ii) a complex between the alkali metal atom and a BT molecule with some additional MP molecules, details of which structures are noted below. However, we at first examine the possibility other than isomer coexistence, on the assumption that only one isomer exists in the present experiment. A PIE curve for $Na(NH_3)$ reported by Hertel and co-workers also shows a structure with steps, and it was concluded to be due to a vibrationally excited state of intermolecular stretching mode.[29] In the present case, almost all vibrational modes for both isomers are calculated to be located below 3000 cm^{-1}. Only the CH stretching vibrations of methyl and H−C≡C groups are found to have frequencies above 3000 cm^{-1}. These energies are almost a half of the observed energy difference between two rising steps, 6300 cm^{-1} (0.78 eV). Each C−H bond length of cation complexes is almost the same as that of the corresponding neutrals, whereas M−O bond lengths are slightly (0.1−0.2 Å) different between the neutral and cation complexes as shown in Figures 5 and 6. This suggests that the C−H bond stretching vibrations are hardly excited in the photoionization process. Therefore, the observed hump structures cannot be explained by the vibrational excitation. Although vibrational progressions are possibly observed in the present PIE curves, we cannot obtain the clear structures due to such progressions.

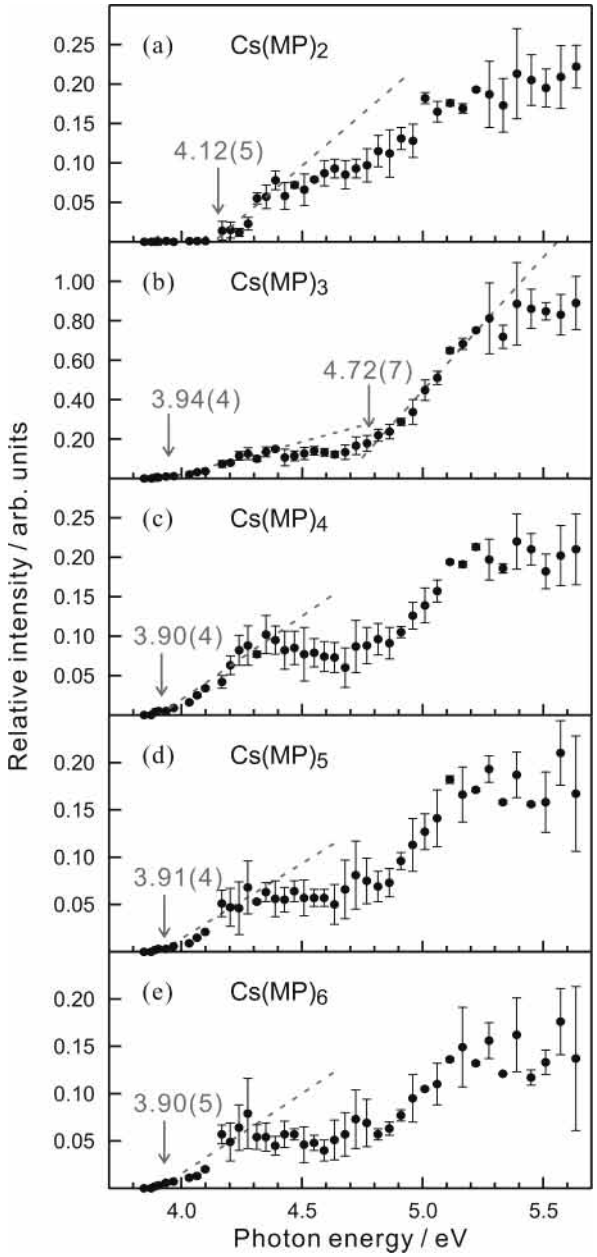

Figure 4. Photoionization efficiency curves for $Cs(MP)_n$ ($n = 2-6$). Two threshold values, which were determined from declines of the curve by using least-squares fitting, are also indicated with arrows. Dashed lines were fitting functions of the least-squares method.

Another possibility for the stepped structures in PIE curves is electronic excitations of the cluster ion. The first excited state of the cesium cation was located at 13.3 eV above the ground state.[35] The excitation energy of the $^1(\pi,\pi^*) \leftarrow S_0$ transition of a methyl benzoate molecule ($C_6H_5COOCH_3$), which is expected to have similar electronic states with the BT molecule, was determined to be 35 926 cm^{-1} (4.45 eV).[36] Thus, the possibility of electronic excitations was excluded in the present observation. Therefore, it is concluded that the step structure in PIE curves is due to existence of several isomers with different ionization energies.

C. Isomers and Ionization Energies. We calculated two types of isomers, (i) solvated $M(MP)_3$ and (ii) reacted M(BT) noted above, based on DFT. Optimized structures of neutral clusters and those of corresponding cations for these isomers of Na and K systems are shown in Figures 5 and 6 for isomers i and ii, respectively. For the neutral solvated isomers, slightly

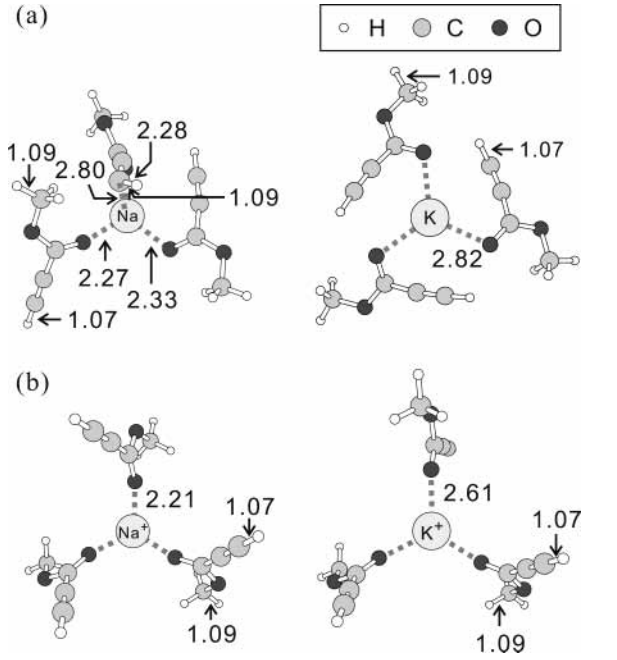

Figure 5. Optimized structures of solvated isomers: (a) neutral complexes of $Na(MP)_3$ and $K(MP)_3$ and (b) cation complexes of $Na^+(MP)_3$ and $K^+(MP)_3$. Intermolecular and C−H bond lengths are shown in Å.

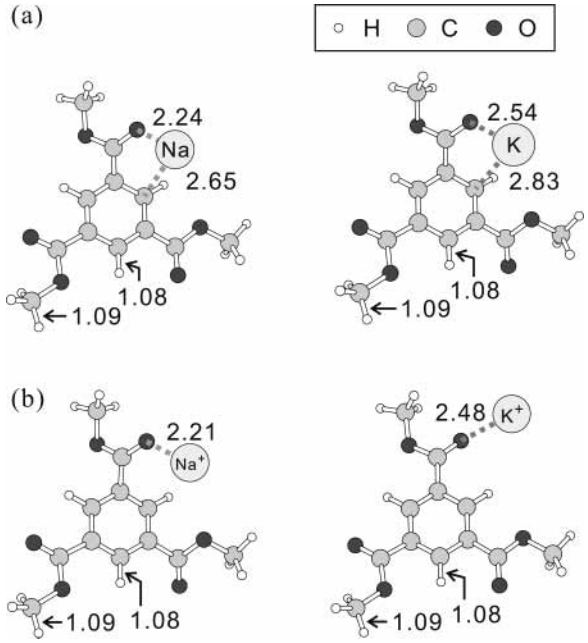

Figure 6. Optimized structures of reacted clusters: (a) neutral complexes of Na(BT) and K(BT) and (b) corresponding cation complexes of Na^+(BT) and K^+(BT). Intermolecular and C−H bond lengths are shown in Å.

different structures were obtained for Na−MP and K−MP clusters; the $K(MP)_3$ complex has a higher symmetric structure than the $Na(MP)_3$; in the latter, one MP molecule was distorted rather than other two MP molecules. However, $Na(MP)_3$ and $K(MP)_3$ have a similar binding nature between a metal atom and MP molecules; each MP molecule is coordinated with the metal atom from the carbonyl oxygen atom. Similar structures with the neutral complexes were obtained in the cation complexes. For the cation, sodium and potassium complexes have similar structures to each other except for intermolecular bond lengths. In the reacted isomers, M(BT), we found two

TABLE 1: Adiabatic Ionization Energies of $M(MP)_3$ Obtained by Density Functional Calculations[a]

	solvated[b]/eV	reacted[b]/eV
Na	3.53	4.24
K	3.27	4.03

[a] Structures of these complexes are shown in Figures 5 and 6. [b] An ionization energy was estimated from the energy difference between neutral and cation complexes without a correction of zero-point vibrational energy.

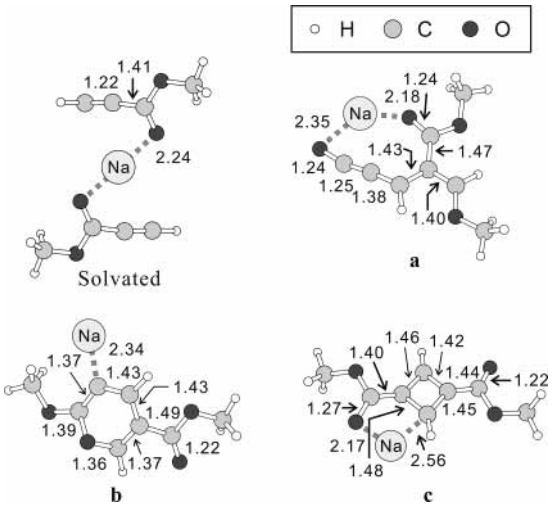

Figure 7. Optimized structures of isomers for $Na(MP)_2$ by the B3LYP/6-311+G(d) level of calculations. Bond lengths are shown in Å.

isomers with different metal coordination sites: (1) a structure in which the metal atom was positioned near the carbonyl oxygen as shown in Figure 6 and (2) a symmetric isomer where a metal atom was located on top of the benzene ring (not shown). The isomer 1 for the K system was found to be 0.26 eV more stable than the isomer 2. Thus we consider ionization energy only for the more stable isomers 1. Calculated adiabatic ionization energies of these reacted and unreacted isomers are summarized in Table 1. For the Na−MP system, the ionization energy of the solvated $Na(MP)_3$ isomer was 0.71 eV lower than that of the reacted Na(BT) isomer. For the K−MP system, the solvated $K(MP)_3$ isomer has also a 0.76-eV lower ionization energy than the reacted isomer. Although the quantitative estimation of ionization energies in the present Cs−MP system is necessary for the comparison with experimental results, it is expected also for the Cs system that the reacted isomer has a higher ionization energy than the solvated isomer. Calculated ionization energy differences between reacted and solvated isomers noted above almost coincide with the observed energy difference between two threshold values. Therefore, we conclude that the higher threshold value of $Cs(MP)_3$, 4.72 eV, corresponds to the reacted Cs(BT) isomer, and the lower value (3.94 eV) is due to the solvated $Cs(MP)_3$ isomer. This is also supported from the fact that the intensity anomaly at $n = 3$ was prominently observed at ionization laser wavelength above 5 eV, whereas the intensity anomaly was insignificant below 4.6 eV.

In the PIE curve of $Cs(MP)_2$, the ion intensity is found to increase monotonically with increasing photon energy, and there is no clear feature for the structural isomers as observed for $n \geq 3$ clusters. Several structural isomers, such as a solvated isomer and a reacted cluster with a cyclic or a linear structure, possibly exist also in the $n = 2$ cluster. Optimized structures for isomers of $Na(MP)_2$ are shown in Figure 7. Structures of polymerized products were optimized from the possible 1,4-addition products of the MP dimer. We estimated ionization energies for these isomers of the $n = 2$ cluster as summarized in Table 2. The ionization energy of the solvated isomer (4.25 eV) is comparable with the observed ionization threshold of $Cs(MP)_2$ (4.12 eV), although the metal atom is different. For K−MP and Na−MP systems, ionization thresholds for $n = 3$ were experimentally determined to be 4.69[37] and 4.49 eV,[28] respectively, of which values are expected to correspond to thresholds for the reaction product, M(BT). This result suggests that the ionization energy of these clusters does not sensitively depend on the nature of alkali metal atoms. The reacted isomers **a**−**c** are found to have higher ionization energies than the solvated isomer. Thus we anticipate that the reacted isomers coexist in $Cs(MP)_2$, because its ion intensity monotonically increases with increasing photon energy up to 5.6 eV. In the $n = 3$ case, polymerized products with linear structures are also possible to coexist, although these structures are not yet examined theoretically at present. From the results of the $n = 2$ cluster, such an isomer is expected to have an ionization energy between those of the solvated and the reacted isomer with the cyclic structure. However, such a tendency was hardly obtained in the PIE curve for $n = 3$. Thus we can consider that the linear isomers of reaction products barely exist in the case of $n = 3$.

TABLE 2: Adiabatic Ionization Energies of Several Structural Isomers for $Na(MP)_2$ Obtained by B3LYP/6-311+G(d) Calculations[a]

		reacted		
	solvated	isomer **a**	isomer **b**	isomer **c**
ionization energy[b]/eV	4.25	4.71	5.03	5.50

[a] Structures of the isomers are shown in Figure 7. [b] An ionization energy was estimated from the energy difference between neutral and cation complexes without a correction of the zero-point vibrational energy.

For $n = 3$, flat regions of relative intensities are clearly observed for both isomers. Relative intensities in the flat regions are expected to reflect the relative abundance of these isomers. From the least-squares fitting of the flat regions, the relative intensity ratio is estimated to be [solvated]/[reacted] = 0.15/0.85. This result indicates that the benzene formation reaction proceeds efficiently in the present condition.

D. Comparison of Two Types of Alkali Metal Sources. In the laser vaporization method, metal atoms are possibly produced with high kinetic energy.[38] In addition, excited metal atoms may also be generated.[39] We examined effects of the laser vaporization method to intracluster anionic polymerization, although high kinetic energy of atoms is expected to be cooled by multiple collisions with helium buffer gas in the present condition. By using a high-temperature pulse valve as a metal source, the mean kinetic energy of an alkali metal atom can be suppressed to several hundreds of meV, whereas kinetic energy distribution of magnesium monocations produced by the laser vaporization was reported to have a maximum at several eV.[38] For both spectra produced by the laser vaporization (Figure 2b) and by the high-temperature pulse valve (Figure 3a), intensity anomalies at $n = 3$ were clearly observed, which indicate intracluster anionic polymerization to produce the BT molecule. Therefore the polymerization of MP molecules proceeds in a thermal condition in the crossed beam configuration. Similar results in the intensity anomaly were also observed in the K−acrylonitrile system, in which intracluster anionic polymerization produces cyclohexane derivatives.[40] Thus, we conclude that the intracluster anionic polymerization initiated by the alkali

metal atom proceeds in the ground state with little kinetic energy effect of the clusters.

Conclusion

The reaction product in clusters containing an alkali metal atom (Na, K, and Cs) and MP molecules have been examined from the results of PIE curve measurements for Cs−MP clusters and DFT calculations for Na−MP and K−MP systems. An intensity anomaly at $n = 3$ was commonly observed in the photoionization mass spectra of $M(MP)_n$ in both types of alkali metal sources, the laser vaporization source and the high-temperature pulse valve. This feature was due to the intracluster cyclotrimerization reaction producing benzene derivatives. Furthermore, a structure in the PIE curve for $n = 3$ was significantly different from that for $n = 2$; two ionization thresholds were discerned in the PIE curve of $n = 3$, whereas one ionization threshold can clearly be determined for $n = 2$. In the present system, two types of isomers are expected to exist for $n = 3$: an alkali metal atom solvated with MP molecules and a complex between an alkali metal atom and the benzene derivative that is a reaction product of intracluster polymerization. From the results of theoretical calculations, the solvated isomer was found to have a lower ionization energy than the reacted isomer, and the difference of ionization energies between two isomers was estimated to be ~0.7 eV for K−MP and Na−MP systems. This value is almost the same as the observed energy difference between two ionization thresholds of $Cs(MP)_3$. Therefore, the high ionization threshold for $Cs(MP)_3$ (4.72 eV) is concluded to originate from the reacted isomer, and the lower threshold value corresponds to the solvated isomer. In addition, the relative intensity of the reacted isomer for $n = 3$ was several times larger than that of the unreacted one. This indicates that the intracluster polymerization producing the benzene derivative proceeds efficiently in the present system.

Acknowledgment. The authors thank to the Computer Center of the Institute for Molecular Science for the provision of the Fujitsu VPP5000 computer. This work has been supported in part by a Grant-in-Aid for Scientific Research from the Japanese Ministry of Education, Science, Sports and Culture. Financial support from Mitsubishi Foundation is also acknowledged. H.T. is supported by the Research Fellowship of the Japan Society for the Promotion of Science for Young Scientists.

References and Notes

(1) For example, see: Saito, S.; Yamamoto, Y. *Chem. Rev.* **2000**, *100*, 2901. Lautens, M.; Klute, W.; Tam, W. *Chem. Rev.* **1996**, *96*, 49. Trost, B. M. *Angew. Chem., Int. Ed. Engl.* **1995**, *34*, 259. Grotjahn, D. B. In *Comprehensive Organometalic Chemistry II*; Hegedus, L. S., Abel, E. W., Stone, F. G. A., Wilkinson, G., Eds.; Pergamon Press: Oxford, 1995; Vol. 12, pp 741−770. Shore, N. E. In *Comprehensive Organic Synthesis*; Trost, B. M., Fleming, I., Eds.; Pergamon Press: Oxford, 1991; Vol. 5, pp 1129−1162.

(2) Reppe, W.; Schlichting, O.; Klager, K.; Toepel, T. *Liebigs Ann. Chem.* **1948**, *560*, 3. Reppe, W.; Schweckendiek, W. *Liebigs Ann. Chem.* **1948**, *560*, 104.

(3) *The Chemistry of Triple-Bonded Functional Groups*; Patai, S., Ed.; Wiley: Chichester, 1994; Supplement C2.

(4) For reviews, see: Chin, C. S.; Won, G.; Chong, D.; Kim, M.; Lee, H. *Acc. Chem. Res.* **2002**, *35*, 218. Rosenthal, U.; Pellny, P.-M.; Kirchbauer, F. G.; Burlakov, V. V. *Acc. Chem. Res.* **2000**, *33*, 119. Bruneau, C.; Dixneuf, P. H. *Acc. Chem. Res.* **1999**, *32*, 311. Chen, J.-T. *Coord. Chem. Rev.* **1999**, *190−192*, 1143. Bruce, M. I. *Chem. Rev.* **1998**, *98*, 1797.

(5) For example, see: Lambert, R. M.; Ormerod, R. M. In *Surface Reactions*; Madix, R. J., Ed.; Springer: Berlin, 1994; Vol. 34, pp 89−144. Abdelrehim, I. M.; Thornburg, N. A.; Sloan, J. T.; Caldwell, T. E.; Land, D. P. *J. Am. Chem. Soc.* **1995**, *117*, 9509. Abdelrehim, I. M.; Caldwell, T. E.; Land, D. P. *J. Phys. Chem.* **1996**, *100*, 10265.

(6) For the reaction mechanism of the Reppe reaction, see: Kirchner, K.; Calhorda, M. J.; Schmid, R.; Veiros, L. F. *J. Am. Chem. Soc.* **2003**, *125*, 11721. Shore, N. E. *Chem. Rev.* **1988**, *88*, 1081. Wakatsuki, Y.; Nomura, O.; Kitaura, K.; Morokuma, K.; Yamazaki, H. *J. Am. Chem. Soc.* **1983**, *105*, 1907. Hardesty, J. H.; Koerner, J. B.; Albright, T. A.; Lee, G.-Y. *J. Am. Chem. Soc.* **1999**, *121*, 6055. Yamamoto, Y.; Arakawa, T.; Ogawa, R.; Itoh, K. *J. Am. Chem. Soc.* **2003**, *125*, 12143. Asao, N.; Nogami, T.; Lee, S.; Yamamoto, Y. *J. Am. Chem. Soc.* **2003**, *125*, 10921.

(7) Schröder, D.; Sülzle, D.; Hrušák, J.; Böhme, D. K.; Schwarz, H. *Int. J. Mass Spectrom. Ion Processes* **1991**, *110*, 145.

(8) Wesendrup, R.; Schwarz, H. *Organometallics* **1997**, *16*, 461.

(9) Schnabel, P.; Irion, M. P.; Weil, K. G. *J. Phys. Chem.* **1991**, *95*, 9688.

(10) Berg, C.; Kaiser, S.; Schindler, T.; Kronseder, C.; Niedner-Schatteburg, G.; Bondybey, V. E. *Chem. Phys. Lett.* **1994**, *231*, 139.

(11) Heinemann, C.; Cornehl, H. H.; Schwarz, H. *J. Organomet. Chem.* **1995**, *501*, 201.

(12) Abbet, S.; Sanchez, A.; Heiz, U.; Schneider, W.-D.; Ferrari, A. M.; Pacchioni, G.; Rösch, N. *J. Am. Chem. Soc.* **2000**, *122*, 3453.

(13) Ferrari, A. M.; Giordano, L.; Pacchioni, G.; Abbet, S.; Heiz, U. *J. Phys. Chem. B* **2002**, *106*, 3173.

(14) Coolbaugh, M. T.; Whitney, S. G.; Vaidyanathan, G.; Garvey, J. F. *J. Phys. Chem.* **1992**, *96*, 9139.

(15) Whitney, S. G.; Coolbaugh, M. T.; Vaidyanathan, G.; Garvey, J. F. *J. Phys. Chem.* **1991**, *95*, 9625.

(16) Tsukuda, T.; Kondow, T. *J. Am. Chem. Soc.* **1994**, *116*, 9555.

(17) Tsukuda, T.; Terasaki, A.; Kondow, T.; Scarton, M. G.; Dessent, C. E.; Bishea, G. A.; Johnson, M. A. *Chem. Phys. Lett.* **1993**, *201*, 351.

(18) Fukuda, Y.; Tsukuda, T.; Terasaki, A.; Kondow, T. *Chem. Phys. Lett.* **1996**, *260*, 423.

(19) Ichihashi, M.; Tsukuda, T.; Nonose, S.; Kondow, T. *J. Phys. Chem.* **1995**, *99*, 17354.

(20) Fukuda, Y.; Tsukuda, T.; Terasaki, A.; Kondow, T. *Chem. Phys. Lett.* **1995**, *242*, 121.

(21) Tsukuda, T.; Kondow, T.; Dessent, C. E.; Bailey, C. G.; Johnson, M. A.; Hendricks, J. H. Lyapustina, S. A.; Bowen, K. H. *Chem. Phys. Lett.* **1997**, *269*, 17.

(22) Ohshimo, K.; Misaizu, F.; Ohno, K. *J. Chem. Phys.* **2002**, *117*, 5209.

(23) Ohshimo, K.; Tsunoyama, H.; Misaizu, F.; Ohno, K. *Eur. Phys. J. D* **2001**, *16*, 107.

(24) Tsunoyama, H.; Ohshimo, K.; Misaizu, F.; Ohno, K. *J. Am. Chem. Soc.* **2001**, *123*, 683.

(25) Tsunoyama, H.; Ohshimo, K.; Misaizu, F.; Ohno, K. *J. Phys. Chem. A* **2001**, *105*, 9649.

(26) Furuya, A.; Ohshimo, K.; Tsunoyama, H.; Misaizu, F.; Ohno, K. *J. Chem. Phys.* **2003**, *118*, 5456.

(27) Ohshimo, K.; Misaizu, F.; Ohno, K. *Eur. Phys. J. D* **2003**, *24*, 339.

(28) Tsunoyama, H.; Ohshimo, K.; Misaizu, F.; Ohno, K. *Int. J. Mass Spectrom.* **2004**, *232*, 41.

(29) Schulz, C. P.; Haugstätter, R.; Tittes, H. U.; Hertel, I. V. *Z. Phys. D: At., Mol. Clusters* **1988**, *10*, 279.

(30) Schulz, C. P.; Haugstätter, R.; Tittes, H. U.; Hertel, I. V. *Phys. Rev. Lett.* **1986**, *57*, 1703.

(31) Misaizu, F.; Sanekata, M.; Tsukamoto, K.; Fuke, K. *J. Phys. Chem.* **1992**, *96*, 8259.

(32) Okunishi, M.; Yamanouchi, K.; Tsuchiya, S. *Chem. Lett.* **1989**, 393.

(33) Frisch, M. J.; Trucks, G. W.; Schlegel, H. B.; Scuseria, G. E.; Robb, M. A.; Cheeseman, J. R.; Zakrzewski, V. G.; Montgomery, J. A., Jr.; Stratmann, R. E.; Burant, J. C.; Dapprich, S.; Millam, J. M.; Daniels, A. D.; Kudin, K. N.; Strain, M. C.; Farkas, O.; Tomasi, J.; Barone, V.; Cossi, M.; Cammi, R.; Mennucci, B.; Pomelli, C.; Adamo, C.; Clifford, S.; Ochterski, J.; Petersson, G. A.; Ayala, P. Y.; Cui, Q.; Morokuma, K.; Malick, D. K.; Rabuck, A. D.; Raghavachari, K.; Foresman, J. B.; Cioslowski, J.; Ortiz, J. V.; Stefanov, B. B.; Liu, G.; Liashenko, A.; Piskorz, P.; Komaromi, I.; Gomperts, R.; Martin, R. L.; Fox, D. J.; Keith, T.; Al-Laham, M. A.; Peng, C. Y.; Nanayakkara, A.; Gonzalez, C.; Challacombe, M.; Gill, P. M. W.; Johnson, B. G.; Chen, W.; Wong, M. W.; Andres, J. L.; Head-Gordon, M.; Replogle, E. S.; Pople, J. A. *Gaussian 98*, revision A.11.1; Gaussian, Inc.: Pittsburgh, PA, 1998.

(34) Becke, A. D. *J. Chem. Phys.* **1993**, *98*, 5648.

(35) Moore, C. E. *Atomic Energy Levels*; United States Department of Commerce, National Bureau of Standards; Washington, DC, 1949; Vol. I.

(36) Kamei, S.; Abe, H.; Mikami, N.; Ito, M. *J. Phys. Chem.* **1985**, *89*, 3636.

(37) Tsunoyama, H.; Misaizu, F.; Ohno, K. Unpublished results.

(38) Sanekata, M.; Misaizu, F.; Fuke, K.; Iwata, S.; Hashimoto, K. *J. Am. Chem. Soc.* **1995**, *117*, 747.

(39) Yasuike, T.; Nakajima, A.; Yabushita, S.; Kaya, K. *J. Phys. Chem. A* **1997**, *101*, 5360.

(40) Tsunoyama, H.; Nakagawara, W.; Misaizu, F.; Ohno, K. Unpublished results.